Nanoscale

Nanoparticle-mediated co-delivery of inflammasome inhibitors provide protection against sepsis

Journal:	*Nanoscale*
Manuscript ID	NR-ART-11-2023-005570.R1
Article Type:	Paper
Date Submitted by the Author:	04-Jan-2024
Complete List of Authors:	Nandi, Dipika; University of Massachusetts Amherst Debnath, Maharshi; University of Massachusetts Amherst, Chemical Engineering Forster, James; University of Massachusetts Amherst, Pandey, Ankit; University of Massachusetts Amherst, Department of Veterinary and Animal Sciences Kulkarni, Ashish; University of Massachusetts Amherst, Chemical Engineering

Nanoparticle-mediated co-delivery of inflammasome inhibitors provide protection against sepsis

Dipika Nandi [1, 2], Maharshi Debnath [1], James Forster III [1], Ankit Pandey [2], Ashish Kulkarni [1, 2, 3, 4]*

[1]Department of Chemical Engineering, University of Massachusetts Amherst, MA, USA

[2]Department of Veterinary and Animal Sciences, University of Massachusetts Amherst, MA, USA

[3]Department of Biomedical Engineering, University of Massachusetts Amherst, MA, USA

[4]Center for Bioactive Delivery, Institute for Applied Life Sciences, University of Massachusetts, Amherst, MA, USA

*Corresponding Author: akulkarni@engin.umass.edu

ABSTRACT:

The NLRP3 inflammasome, a multiprotein complex responsible for triggering the release of pro-inflammatory cytokines, plays a crucial role in inducing the inflammatory response associated with sepsis. While small molecule inhibitors of NLRP3 inflammasome have been investigated for sepsis management, delivering NLRP3 inhibitors has been accompanied by several challenges, primarily related to drug formulation, delivery route, stability, and toxicity. Many existing inflammasome inhibitors either show higher liver toxicity or require a high dosage to efficiently impede inflammasome complex assembly. Moreover, the potential synergistic effects of combining multiple inflammasome inhibitors in sepsis therapy remain largely unexplored. Therefore, a rational approach is essential for presenting the potential administration of NLRP3 small molecule inhibitors to inhibit NLRP3 inflammasome activation effectively. In this context, we present a lipid nanoparticle-based dual drug delivery system loaded with MCC 950 and Disulfiram, demonstrating markedly higher efficiency compared to an equivalent amount of free drug combinations and individual drug nanoparticles *in vitro*. This combination therapy substantially improved the *in vivo* survival rate of mice for LPS induced septic peritonitis. Additionally, the synergistic approach illustrated a significant reduction in the expression of active caspase 1 as well as IL-1β inhibition integral components in the NLRP3 pathway. This study underscores the importance of integrating combination therapies facilitated by nanoparticle delivery to address the limitations of small molecule inflammasome inhibitors.

KEYWORDS:

Inflammasome, co-delivery, lipid nanoparticles, peritonitis, MCC950, Disulfiram.

INTRODUCTION

Sepsis is a complex and life-threatening medical condition resulting from an imbalance in the host-immune response following an infection. It could lead to several complications such as systemic inflammation, hypotension, organ dysfunction, and, in severe cases, death[1,2]. Despite significant advancements in critical care and therapies, sepsis still poses a substantial mortality threat of over 20%, making it the foremost cause of death among ICUs (intensive care units) patients. The management of sepsis poses a formidable challenge due to its multifaceted etiology, rapid pathogenic progression, and the intricacies of achieving an optimal initial therapeutic dose as well as regimen[3,4,5]. Recent studies and discussions within the sepsis research domain have predominantly focused on elucidating the principal determinant of sepsis survival. Central to this discourse is the ongoing debate concerning whether the greater determinant lies in innate and adaptive immune dysfunction or in the delicate equilibrium between inflammatory and anti-inflammatory processes. [6,7]. As inflammatory mediators and proinflammatory cytokines like tumor necrosis factor-alpha (TNF-α), interleukin-1 (IL-1), and interleukin-6 (IL-6) have shown to cause amplified immune responses in sepsis; mitigating the excessive inflammatory response has emerged as a pivotal focal point in sepsis treatment research, as reported by numerous studies[8,9,10]. In line with this, the NLRP3 (nucleotide-binding domain, leucine-rich–containing family, pyrin domain–containing-3) inflammasome has been studied as a potential therapeutic target for sepsis due to its role in regulating the inflammatory response[11,12,13]. The NLRP3 inflammasome activation is a two-step process that mediates caspase-1 activation and the secretion of proinflammatory cytokines IL-1β/IL-18 in response to microbial infection and cellular damage[14–18,]. Literature lists several inflammasome inhibiting drugs that could help alleviate inflammation and be utilized for treating several inflammatory diseases.[19-21]. However, concerns of toxicity, *in vivo* stability, bioavailability, and delivery represent a significant challenge while developing and using anti-inflammatory drugs, especially in treating conditions like sepsis.[22-24] Therefore, given the complexity and diverse manifestations of sepsis, a multifaceted approach addressing multiple aspects of the condition is needed, in order to improve treatment outcomes.

Trials targeting single components of the inflammatory cascade have often failed to significantly reduce multiple organ injury, dysfunction or mortality rates associated with sepsis[10,12,25-27]. In this context, combination therapies can offer a promising approach for targeting multiple components of the NLRP3 inflammasome pathway to treat sepsis[28–30]. Also, nanoparticle-based drug delivery holds great potential for mitigating issues[31–33] related to liver toxicity and high dosage[34] associated with small molecule inhibitors, including those targeting the inflammasome. Nanoparticles can serve as a platform to safely package a rational combination of drugs and ensure their efficient delivery[35,36]. In this manner, the combination drugs can exhibit synergistic effects by inhibiting inflammasome-associated components either simultaneously or sequentially by following horizontal or vertical inhibition. In addition, liposomes will also ensure increased retention time of drugs and their sustained release over time, reducing the need for a repeated high dosage of free drugs and their several off-target effects[37,38]. Thus, we hypothesized that co-delivery of rationally combined inflammasome-inhibiting drugs via nanoparticle platform offers synergistic therapy due to enhanced retention of drugs acting simultaneously on several targets participating in the inflammasome signaling pathway. Here, we proposed to simultaneously deliver a combination of NLRP3 complex inhibitor MCC-950[39-42] and Gasdermin D inhibitor disulfiram[43-46] drug using a 1,2-dioleoyl-sn-glycero-3-phosphocholine (DOPC) lipid nanoparticle[37] system which will ensure their increased solubility, enhanced bioavailability, and increased retention time in circulation.

In this study, we first synthesized and characterized single drug nanoparticle systems, MCC Np and DSR Np and tested their efficiency to inhibit IL-1β along with their respective free drugs. We found single drug nanoparticles to be as efficient as that of the respective equivalent amount of free drugs at later time points, especially after 10 hr, even at a lower dose of 100 nM of drug. After identifying the optimum time points and concentrations we next synthesized dual drug loaded nanoparticle MCC-DSR Np (***Figure-1A***) and analyzed their kinetics for IL-1β inhibition in comparison to that of combination of equivalent free drugs and single drug nanoparticles. The dual drug nanoparticle could internalize efficiently in macrophages (***Figure-1B***) and cause sustained release of both the drugs (***Figure-1C***), thus making MCC-DSR Np to be

the most efficient platform among all other platforms after 24 hr of treatment. MCC-950 prevents the NLRP3 oligomerization (***Figure-1D***) and disulfiram acts on Gasdermin-D to prevent pore formation on the cell surface, thus inhibiting IL-1β release (***Figure-1E***). These dual effects were confirmed by studying the expression of active caspase-1 and IL-1β cytokine release, anticipated to exhibit a direct influence due to the activity of individual drugs. Additionally, we tested these nanoparticles in LPS induced peritonitis animal model to identify their in-vivo efficacy and found that MCC-DSR co-encapsulated nanoparticles were able to provide complete protection against LPS-mediated sepsis through their synergistic response (***Figure-1F***).

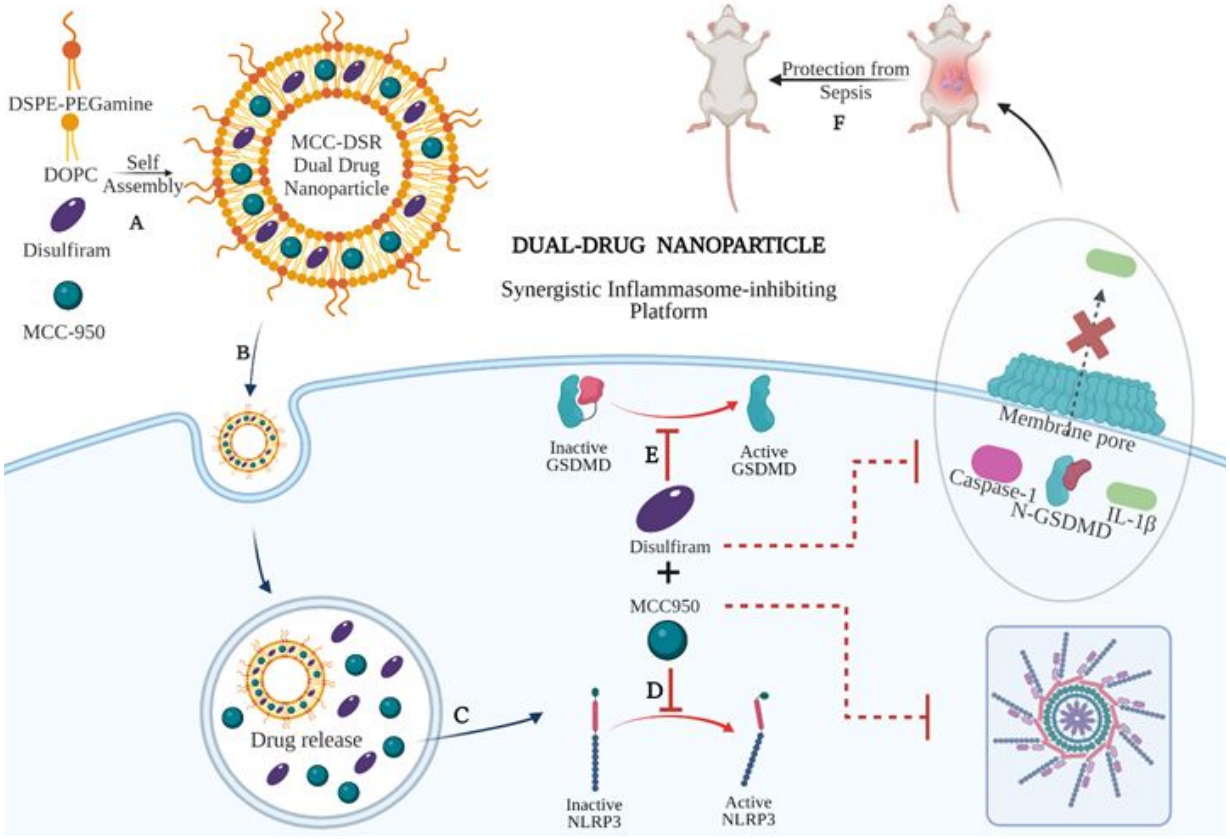

Figure 1. Schematic showing the synergistic therapeutic platform for Dual-Drug Nanoparticle. (**A**) Self Assembly of DSPE-PEG Amine, DOPC lipids along with MCC-950 (NLRP3 inhibitor) and Disulfiram (Gasdermin D inhibitor) for the synthesis of dual drug lipid nanoparticle system (**B**) Internalization of MCC-DSR Np in macrophages (**C**) Release of the drugs MCC-950 and Disulfiram inside the endosome (**D**) MCC-950 binds to NLRP3 and prevents its oligomerization and thus inhibits the activation of NLRP3 inflammasome complex (**E**) Disulfiram blocks the activation of Gasdermin D which prevents the pore formation and the subsequent release of cytokines outside the cell. (**F**) Dual-drug nanoparticle system provides protection against LPS induced sepsis in mice.

RESULTS & DISCUSSION:

Synthesis and Characterization of single and dual inflammasome-inhibiting drug nanoparticles

We first synthesized single and dual drug nanoparticles by utilizing co-lipid nanoparticle backbone obtained from 60 mole percent of DOPC lipid (1,2-Dioleoyl-sn-glycero-3-phosphocholine) and 30 mole percent of DSPE-PEG(2000)amine (1,2- distearoyl-sn-glycero-3-phosphoethanolamine-N- [amino (polyethylene glycol)-2000]). The co-lipid bilayer is then physically encapsulated with either MCC-950 or/and disulfiram (DSR) inflammasome inhibiting drugs, accounting for the rest of the 10 mole percent either individually or in combination in order to form single or dual drug nanoparticles. ***Figure-S1*** represents the characterization of the size and stability for MCC950/DSR single drug Np. For MCC-DSR Np, both drugs were encapsulated in the molar ratio of 1:1 with each contributing towards 5 mole percentage. All the nanoparticles were synthesized by thin lipid film hydration method[47], where the thin lipid film obtained via rotavap were hydrated in PBS for 1.5h at 60°C so as to allow their self-assembling into lipid bilayer along with entrapment of the drugs[48]. The encapsulation efficiency of disulfiram accounted for around 60% whereas that of MCC was around 20%[49]. All the drug nanoparticles; DSR Np, MCC Np and MCC-DSR Np were stably formed and had a hydrodynamic diameter less than 200 nm. ***Figure-2A*** shows the hydrodynamic diameter of MCC-DSR Np to be around 150 nm, obtained via dynamic light scattering using Malvern Nano Zetasizer. The size and morphology of these liposomes were also confirmed using cryo-TEM as shown in ***Figure-2B***. These dual drug nanoparticles were found to be stable in 10% human serum for about 48h with almost no change in size and zeta potential (***Figure-2C***). They were also stable in storage conditions of PBS at 4°C for about a month with size maintained at almost 150 nm and neutral surface charge (***Figure-2D***). Next, we determined the macrophage internalization of these particles by encapsulating FITC at 5 mole percent to obtain fluorescent nanoparticles detectable by microscopy and flow cytometry. ***Figure-2E*** represents the microscopic images of time-dependent cellular uptake of FITC Np from 0h to 8h. ***Figure-2F*** displays the quantification of FITC nanoparticle internalization at different time points using microscopy and it shows that the internalization increased with higher time points, with

4-8 hours showing sufficient internalization for later studies. ***Figure-2G*** plots the concentration dependent internalization of these fluorescent particles showing increasing uptake with higher concentration. Overall, these results show that the drug encapsulating liposomes were stably synthesized and successfully internalized by immortalized macrophages in a concentration and time-dependent manner.

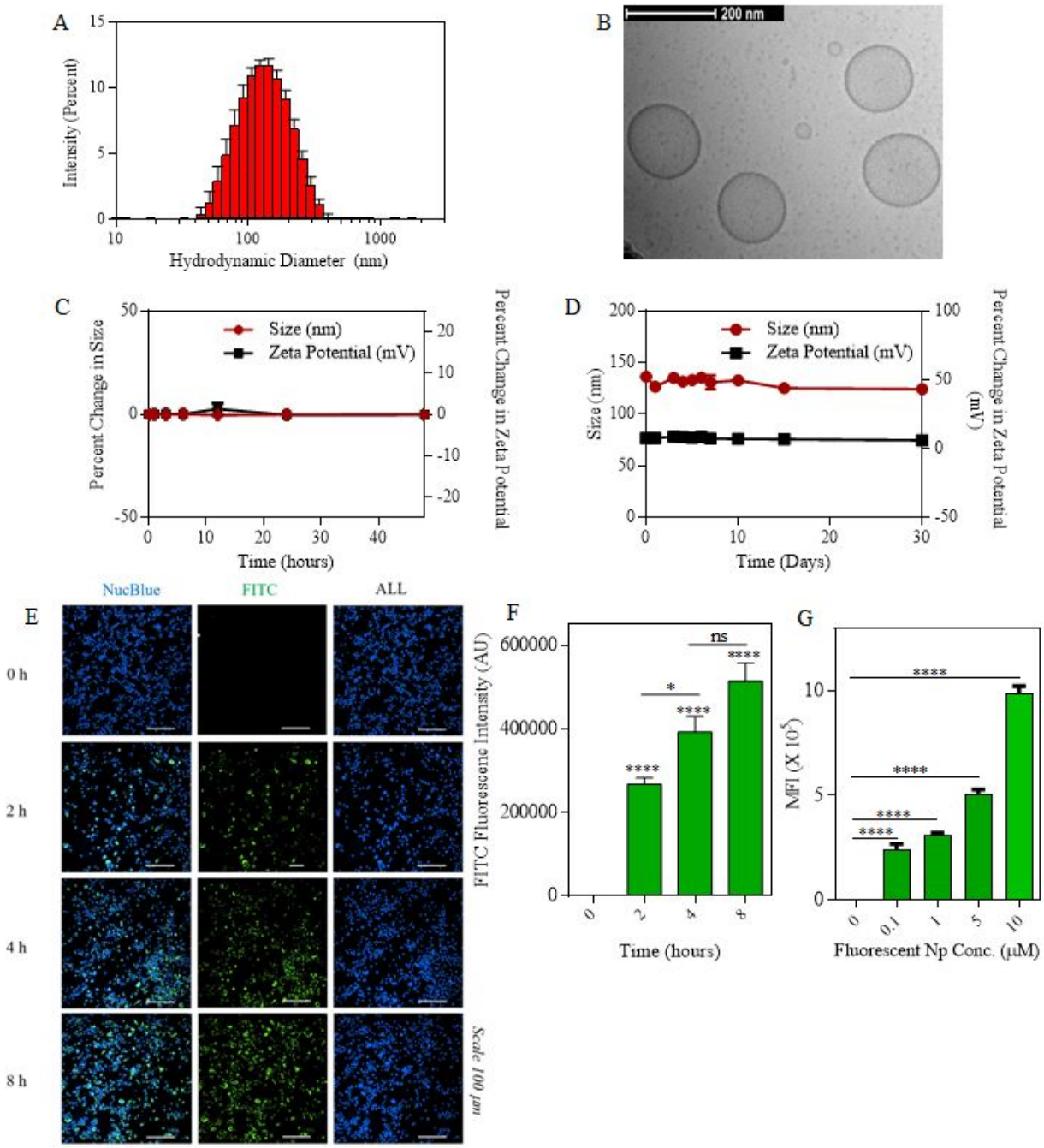

Figure-2: MCC-DSR Np characterization and internalization. (**A**) Graph plots the hydrodynamic diameter of MCC-DSR dual drug nanoparticle. Data shown as mean ± S.D. (n=3). (**B**) CryoTEM image of dual drug nanoparticle. Scale bar: 200 nm. (**C**) Graph displays the percentage change in size and zeta potential of MCC-DSR dual Np incubated in human serum for a total duration of 48hours. (**D**) PBS Stability plot shows size and zeta potential of MCC-DSR Np in PBS over a period of 30 days. Data shown in c and d are mean ± S.E.M. (n=3). (**E**) Representative microscopy images of iBMDMs internalized with FITC encapsulated fluorescent particles in a time-dependent manner from 0h to 8h. Nuclei were stained with NucBlue. Scale bar: 100 μm. (**F**) Quantitative analysis for cellular uptake of fluorescent nanoparticles imaged via confocal microscopy. (**G**) Flow cytometry analysis of cellular uptake of different concentrations of 5FAM particles by iBMDMs. Data shown is mean ± S.E.M. (n=3). Statistical analysis was performed by one-way ANOVA and Dunnett's multiple comparisons test. *p < 0.05, **p < 0.01, ***p<0.001.

Single drug nanoparticles display efficient IL-1β inhibition as compared to free drug overtime at different concentrations.

We next proceeded towards examining if the nanoparticles are as efficacious as that of free drug and their kinetics as well as response at different time points and concentrations. In order to do that, we first primed the immortalized macrophages for 2hr and then treated them with either free drug or nanoparticle for a maximum of 4hr (***Figure-3A***). After 4hr, the cells were replaced with fresh LPS media and allowed to incubate for the next 14hr. This treatment was further proceeded towards signal 2 nigericin at different time points starting from 0hr to 18hr immediately after the LPS priming. The indicated time points of 0, 2, 4, 6, 8, 11, 14 and 18 represent the total nanoparticle treatment and incubation time points at which nigericin was added to different wells in order to activate inflammasome. The assays were performed such that all the different time point treatments end at the same time so as to add nigericin to all the wells exactly at one time point. For this the initial set up or treatments were performed at different time points so as to ensure these variations as mentioned above. After 1hr of nigericin treatment the supernatant was collected and tested for IL-1β levels using ELISA. Before nigericin treatment, the cells were subjected to MTT assay so as to determine the cytotoxicity of the nanoparticle and free drug in order to determine if the IL-1β inhibition is solely via drug's activity. Both ***Figure-3C*** and ***Figure-4A*** show that at later time points even 100 nM of nanoparticle shows a similar response to that of free drug. Even if at initial time points free drug seem to be more efficacious in IL-1β inhibition at certain concentrations, there is no significant difference in the

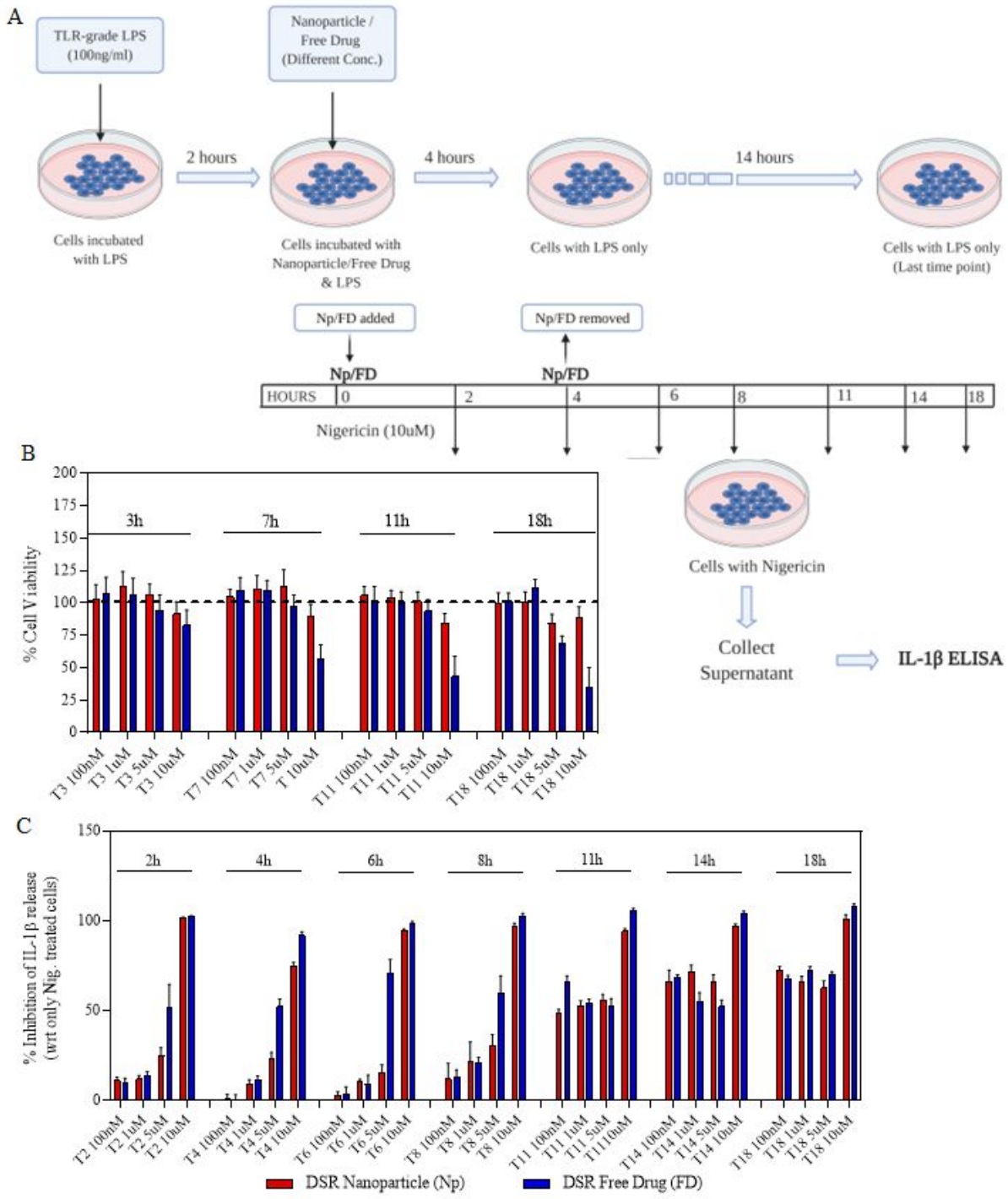

Figure 3. DSR Np activity and cytotoxicity. (**A**) Schematic illustration of sequence and time points for different treatments of single drug or nanoparticles; including LPS, Nanoparticle or Free drug, followed by nigericin. (**B**) Percent cell viability of cells treated with different concentrations of DSR Np or free drug, treated for different time duration. (**C**) Concentration and time-wise percent inhibition in IL-1β stimulation after treating the cells with either DSR Np or DSR free drug. Data shown in (**B**) & (**C**) are mean ± S.E.M. (n=3).

activity at later time points. Moreover, ***Figure-3B*** and ***Figure-4B*** show that free drug is toxic at higher concentration and later time points in case of both MCC-950 and DSR, whereas all the nanoparticles

maintain the cell viability of 80-90% which makes them more efficient than free drug due to sustained release of drug, thus, reducing their toxicity. After determining the single drug nanoparticle efficacy over the respective free drug, we next proceeded towards examining the activity of dual-drug nanoparticles.

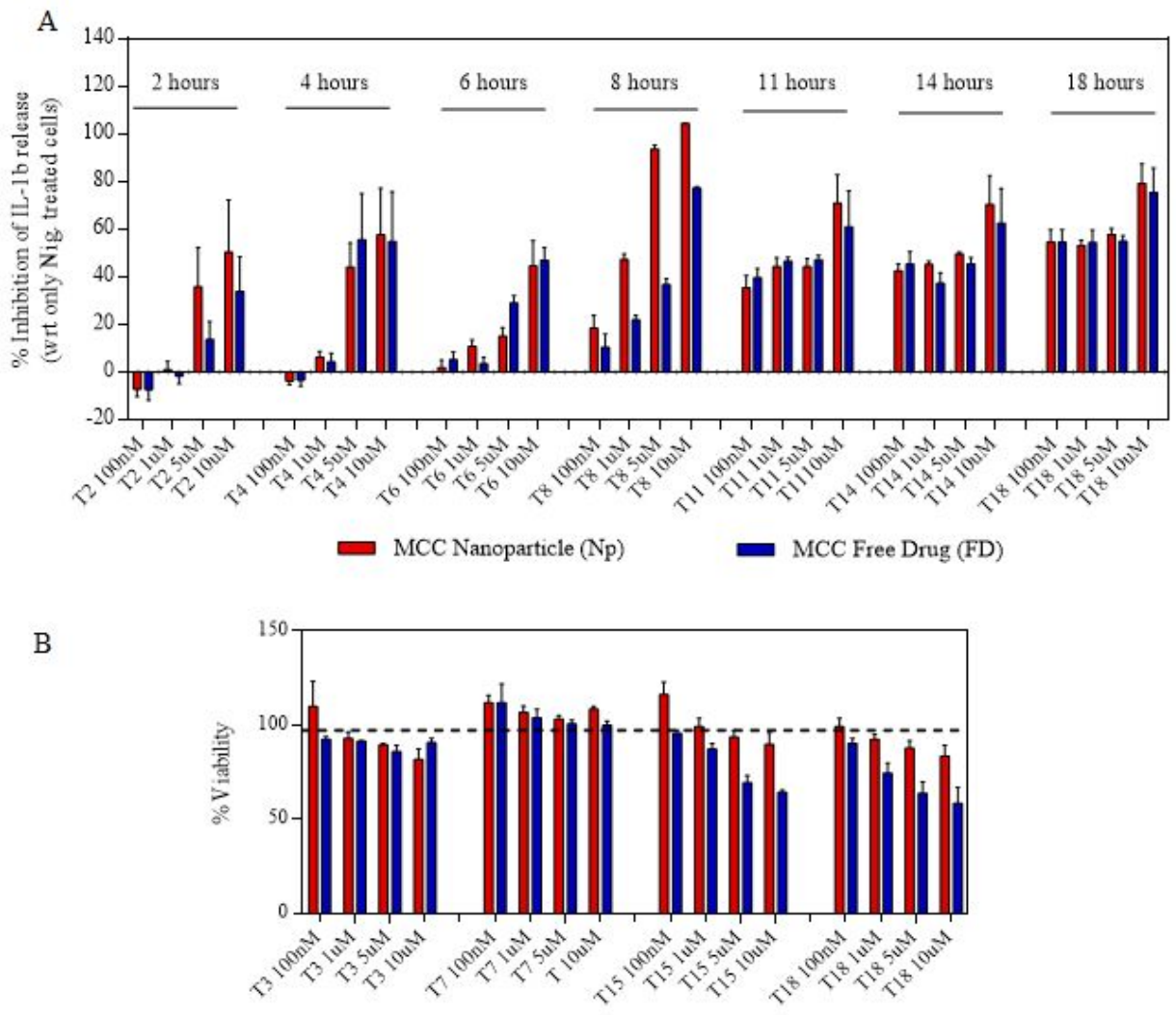

Figure 4. MCC Np activity and cytotoxicity. (**A**) Concentration and time-wise percent inhibition in IL-1β stimulation after treating the cells with either MCC Np or MCC free drug. (**B**) Percent cell viability of cells treated with different concentrations of MCC Np or free drug, treated for different time duration. Data shown in (**A**) & (**B**) are mean ± S.E.M. (n=3).

Dual drug nanoparticles show a synergistic inhibition in IL-1β release in nigericin treated iBMDMs

Next, we examined the efficacy of MCC-DSR Dual Np with respect to dual free drug and single drug Np at different time points ranging from 4hr to 36hr. The time points represent the total time of 4hr nanoparticle treatment and incubation afterwards. For example, 8 hr time point means that the cells were incubated with nanoparticle or free drug for 4hr and then incubated in LPS media for another 4hr. Similarly, 36 hr represents 4hr nanoparticle or free drug treatment and 32 hr of incubation in LPS media for sustained release. We utilized 344 nM of MCC950 and 1 μM of DSR for all our *in-vitro* experiments by keeping these doses consistent in all the platforms, including dual Np, single drug Np and via free drugs. ***Figure-5A*** plots the percentage inhibition in IL-1β released by different treatment groups with respect to the nigericin treated cells. It shows that even though there is not a significant difference among all the treatment groups until 20 hr, MCC-DSR Np shows greater inhibition in IL-1β starting from 24 hr. At 36 hr, dual Np shows significantly higher response shown by inhibiting IL-1β release, followed by MCC Np, dual free drug and DSR Np, thus pointing towards the greater efficacy of the dual drug nanoparticle due to synergistic properties of both the drugs. To reconfirm this response, we next evaluated the expression of different inflammasome-associated proteins[50] in the cells treated with different free drugs and nanoparticles for 24 hr (4 hr treatment and 20 hr incubation) as indicated in ***Figure-5B***, using western blotting. We determined the protein expression in both cell lysate and supernatant. We observed no significant difference in Pro-caspase-1 expression in cell lysate, but in supernatant both MCC-DSR Np and MCC Np showed significant inhibition in active capsase-1 expression, confirming their better efficacy than the respective free drug treatments. Additionally, we observed a remarkable inhibition in active GSDMD released into supernatant of MCC FD, MCC Np and MCC-DSR Np treated cells, again proving their efficiency in inflammasome inhibition. However, we were not able to observe much difference in DSR Np but were able to observe some inhibition in DSR FD, which might be due to the particular time point we are using for western blotting. We also imaged and quantified the adaptor protein ASC (apoptosis-associated speck-like protein containing a CARD) speck formation in iBMDMs which can be used as a simple upstream readout for inflammasome activation[49,51-55]. The minimal speck generation upon dual drug Np treatment ***(Figure-S4A,***

S4B) indicated the ASC proteins being dispersed in the cytosol and thus correlated with lesser inflammasome activation. This further corroborates our previous findings by exhibiting a significant decrease in NLRP3 inflammasome activation due to the combined effect of the dual-drug nanoparticle.

Dual drug nanoparticles induce complete protection against LPS-induced sepsis

We next examined the *in-vivo* efficacy of dual drug nanoparticle in LPS peritonitis sepsis model. For this, the mice were intraperitoneally injected with 50 mg/kg LPS to induce sepsis systemically (***Figure-5C***). After 1 hr of LPS injection, these mice were intravenously injected with either free drug or nanoparticles and then closely monitored for survival. The doses for MCC950 were 0.4 mg per mice (~2 mg/kg) and that of DSR was 0.8 mg per mice (~4 mg/kg), delivered either via nanoparticle or as free drug. ***Figure-5D*** shows the survival curve for all the treatment groups. We observed that all the mice without any treatment died within 12 hr to 18 hr, however, the survival was extended to 24 hr when the mice were treated with DSR Np. Moreover, one out of five mice managed to survive and recover in both the treatments with MCC Np as well as Dual FD, with Dual FD showing enhanced survival for other mice when compared with just MCC Np. Dual Np showed the maximum survival out of all the treatment groups where four out of five mice survived and fully recovered until later time point, 120 hr. On day 5, all these four mice completely recovered from septic shock and were able to regain their normal weight and movement. All the mice were subjected to peritoneal cell isolation, cardiac puncture and tissue harvesting after their sacrifice. All the mice were closely monitored for their posture, mobility, appearance, and weight loss; and they were all humanely sacrificed as per IACUC guidelines. After sacrificing the mice, the heart, lung, liver, kidney, and spleen were removed and sectioned for hematoxylin & eosin (H&E) staining to assess treatment biosafety as well as the presence of peritonitis from the kidney and spleen samples. **Figure-S5** shows the H&E biosafety results, exhibiting completely normal histology in the PBS No LPS group, as well as the MCC FD and NP groups. The other treatment groups also exhibited healthy histology but with some interesting findings. For example, for the PBS LPS, DSR FD, and DSR NP groups, there was a high presence of

neutrophils in the lungs but only in the surrounding tissue, not in the alveolar sacks, meaning there is no evidence of pneumonia which could result in lung inflammation. In the Dual NP group and slightly less prevalent in the Dual FD group, the spleen exhibited a blue follicle surrounded by normal red tissue with some acute immune cell infiltration (blue spots), indicating the tail-end of an ameliorating inflammatory response. However, in total the H&E biosafety results exhibit largely normal tissue morphologies and do not provide evidence for any significant toxicities from the treatment groups.

The recovered mice were sacrificed on day 5. The isolated peritoneal cells were immediately lysed using RIPA buffer enriched with 1X protease inhibitor and subjected to protein isolation. Later the protein was quantified using BCA Assay and equal amount of protein were loaded and quantified using protein simple Wes. ***Figure-5E*** show the protein expression of p20 Caspase-1 normalized to Pro-Caspase-1 in the peritoneal cells isolated from mice treated with indicated free drugs and nanoparticles. The graph shows significantly higher activation of caspase-1 enzyme in the LPS treatment mice without any drug treatment. And this expression is inhibited by around 40% in MCC + DSR free drug treatment group and 80% in mice treated with MCC-DSR Np, which is remarkably greater than the response obtained from single drug treatments. Moreover, dual-drug liposome treatment group showed almost equivalent levels of active capsase-1 as that of the no-disease control mice (without any LPS injection), proving that these mice were fully recovered from sepsis. We further examined all the treatment groups for serum IL-1β levels and observed a significantly higher level of the cytokine (~1800 pg/ml) in LPS injected mice without any drug treatment (***Figure-5F***). These were sequentially inhibited by treatment with different free drug and nanoparticles, with a 20-fold reduction upon treating the mice with dual-drug Np, showing no serum IL-1β similar to that of no disease control. Additionally, the dual Np also showed significant reduction in IL-6 secretion (***Figure-S2***) without a consequential change in TNFα release (***Figure-S3***), suggesting its potential efficacy in the simultaneous blockade of multiple cytokines, thereby mitigating the cytokine storm often accompanied with sepsis. We also performed sectioning of peritoneal lining tissues to assess the presence of peritonitis by H&E staining and assessment by pathologists. ***Figure-S6*** depicts select H&E stains from

sections taken from peritonitis-positive mainly splenic as well as some liver peritoneum of the septic mice, shown in 10x and 40x magnification to depict the characteristics of immune cell infiltration in peritonitis. The H&Es from each sample were also pathologically assessed for peritonitis in both spleen/kidney sections (***Figure-S6A***), which serve as the most representative for peritoneal lining sections, and in the heart/lung/liver (***Figure-S7B***) of the septic mice tissues. Of particular note is the presence of acute or chronic peritonitis in all groups of the spleen/kidney samples, but no presence of peritonitis is detected in the PBS No LPS (negative control), as well as the Dual FD Sample II and Dual NP groups, suggesting amelioration of sepsis and peritonitis in these tissues, providing further evidence for the effectiveness of the MCC-DSR drug combo, including in the nanoparticle system. Overall, all the *in-vivo* and *ex-vivo* assays support the fact that MCC-DSR Np enable a synergistic response which offers complete protection against LPS-mediated sepsis.

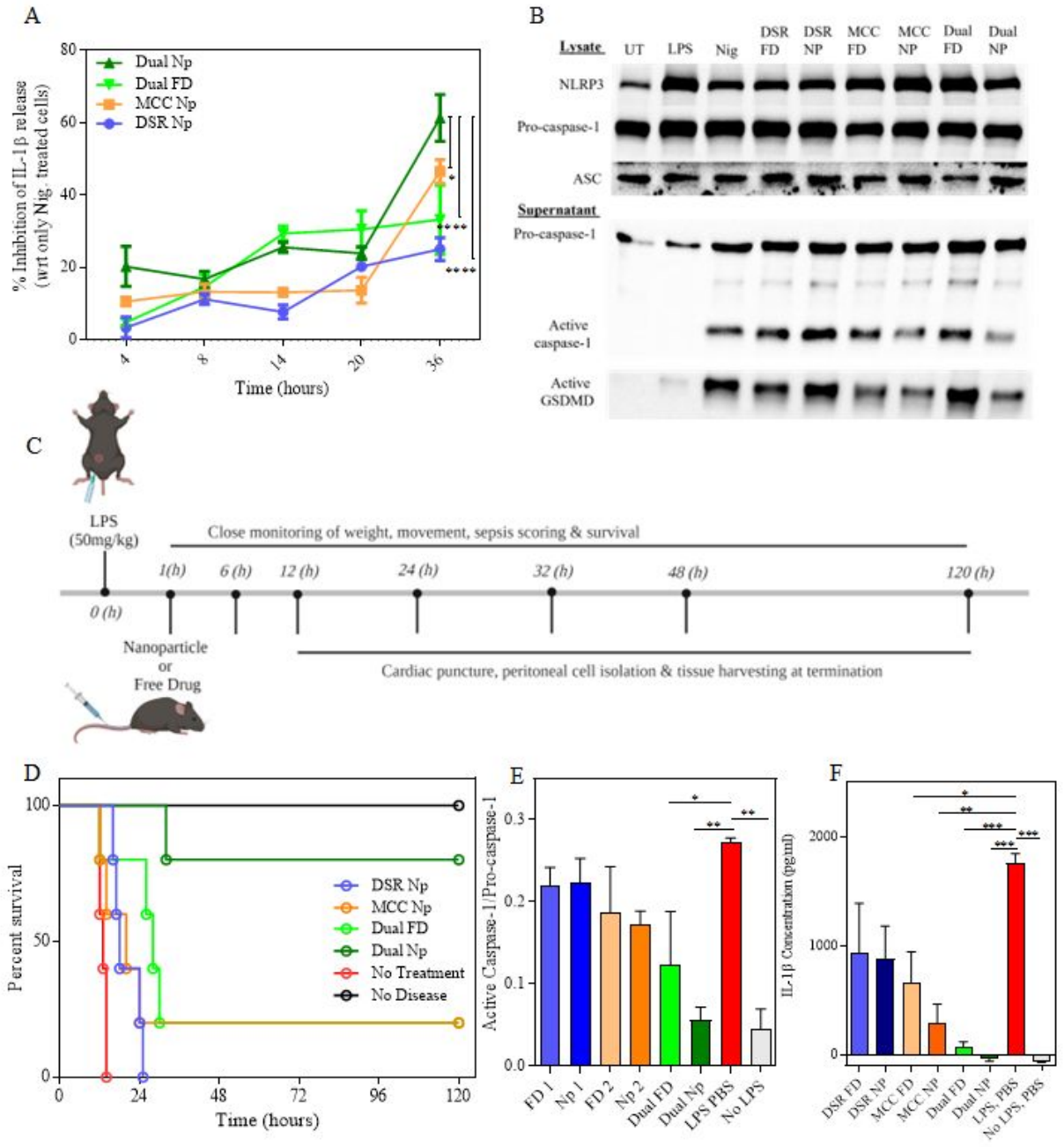

Figure 5. *In-vitro* and *In-vivo* efficacy of dual drug MCC-DSR Np. (**A**) Graph plots the percent IL-1β inhibition conducted by indicated treatment groups, including dual Np, dual FD, MCC Np and DSR Np. Data shown is mean ± S.E.M. (n=3). Statistical analysis was performed by two-way ANOVA and Dunnett's multiple comparisons test. *p < 0.05, ***p<0.001. (**B**) Representative western blotting images of different treatment groups exhibiting the expression of NLRP3 signaling associated proteins in the cell lysate and supernatant. (**C**) Schematics representing *in-vivo* animal trial timeline displaying all the time points and sequence of different treatments and related assays. (**D**) Graph plots the survival curve of indicated treatment groups for a duration of 120hr. (**E**) Graph plots the quantitation of expression of active Caspase-1 normalized to Pro-Caspase-1 observed via simple protein WES analysis. Data shown is mean ± S.E.M. (n=3). Statistical analysis was performed by ordinary one-way ANOVA and Dunnett's multiple comparisons test. *p < 0.05, **p<0.01. (**F**) Graph plots serum IL-1β cytokine levels in the different treatment groups. Data shown is mean ± S.E.M. (n=3). Statistical analysis was performed by ordinary one-way ANOVA and Dunnett's multiple comparisons test. *p < 0.05, **p<0.01, ***p<0.001.

CONCLUSIONS

This study successfully demonstrated stable synthesis of MCC-DSR dual drug nanoparticles of less than 200 nm hydrodynamic diameter and neutral surface charge. These nanoparticles showed remarkable stability in PBS for about 30d and in serum for about 2d. The combination nanoparticle displayed a significantly higher efficiency than equivalent amount of free drug combinations as well as individual drug nanoparticles *in-vitro,* as evidenced by significant IL-1β inhibition after 24h of total treatment. Western blot analysis further corroborated these results revealing a substantial inhibition in active caspase-1 and active GSDMD expression after 24h (4h treatment and 20h incubation) dual nanoparticle treatment in contrast to no inhibition after free drug treatment. Notably, even a mere 1μM of DSR was able to induce sufficient inhibition when delivered along with 344nM of MCC due to synergistic response. This dose is around 10-20 times lower than the previously employed doses of DSR free drug to achieve *in-vitro* pyroptosis inhibition. Furthermore, our study unveiled a remarkably high in-vivo efficiency in LPS-mediated sepsis model, with dual drug Np inducing a complete protection against sepsis even when exposed to a very high LPS dose of 50 mg/kg. The co-delivery of MCC and DSR via combination nanoparticles not only greatly enhanced the survival rates of mice but also facilitated their recovery from severe septic shock to completely normal states. This response not only outperforms other platforms tested simultaneously in this study, but also surpasses the efficacy of high doses of free drugs in previous studies[28,29]. In this study, we employed doses of the GSDMD inhibitor and NLRP3 inhibitor that were 3-10 times lower than those in previous studies, achieving superior results compared to individual drug treeatments[30,31,32]. In conclusion, our results establish that this platform not only offers a synergistic inflammasome inhibitory response which greatly reduces the required individual drug doses but also provides a safe delivery system thereby mitigating toxicity and enabling sustained release overtime, ultimately enhancing drug retention. This study serves as a proof of principle for combinatorial approaches that have the potential to overcome the existing limitations of inflammasome-inhibiting drugs, which have thus far encountered barriers to clinical translation.

MATERIALS AND METHODS

Materials

All the reagents were procured from commercial suppliers including ThermoFisher, InvivoGen, Tocris, Avanti, Adipogen, Biolegend, BioRad, Cell Signaling Technology, Biorad and Sigma Aldrich. Nanoparticle components 1,2-Dioleoyl-sn-glycero-3- phosphocholine (DOPC, Cat# 850375P) and 3-phosphoethanolamine-N-[amine (polyethylene glycol)-2000] (DSPE-PEG2000Amine, Cat# 880128P) were purchased from Avanti Polar Lipids. Disulfiram drug, also known as Bis(diethylthiocarbamyl) disulfide (Cat# 97-77-8), was obtained from Millipore Sigma. MCC-950 Sodium (CP-456773 Sodium) was purchased from Selleckchem. For cell-based assays, all the immortalized bone-marrow-derived macrophages (iBMDMs) including the cell lines expressing ASC-citrine was generously gifted by Kate Fitzgerald, UMass Chan Medical School, Worcester. Cell culture media components such as Dulbecco's modified Eagle's medium (DMEM), fetal bovine serum (FBS), and Penicillin-Step were ordered from Gibco, Life Technologies. For inflammasome stimulation, ultrapure lipopolysaccharide from Escherichia coli (Ultrapure LPS, E.coli 0111:B4, Cat# tlrl-3pelps) and Nigericin sodium salt (Cat# 431210) were obtained from InvivoGen and Tocris Bioscience, respectively. All the western primary and secondary antibodies were procured from Adipogen Life Sciences, Biolegend, Abcam, Santa Cruz Biotechnology and Cell Signaling Technology. Other reagents like RIPA buffer, NP-40 lysis buffer, HALT protease and phosphatase single-use EDTA-free 100X cocktail, J60015 4X Laemmli SDS reducing sample buffer, NucBlue Live Ready Probes Reagent (Hoechst 33342), and LysoTracker Red DND-99 were purchased from ThermoFisher Scientific. Moreover, some kits like IL-1β Mouse Uncoated ELISA and Pierce BCA Protein Assay were also obtained from ThermoFisher Scientific. Wes reagents were procured from Protein Simple.

Detailed Methods

Synthesis of MCC Np, DSR Np and MCC-DSR Np

Both the single and dual drug particles were synthesized using two lipids, DOPC {1,2-Dioleoyl-sn-glycero-3-phosphocholine} and DSPE-PEG(2000)amine 204 at 60 mol percent and 30 mol percent, respectively, using thin lipid film hydration method. Individual or combination of two drugs were physically encapsulated, accounting for a total of 10 mol percent. While preparing the thin film, both the co-lipids and disulfiram were dissolved in dichloromethane, whereas MCC-950 was dissolved in methanol. The film was obtained in a round bottom flask using the rotavapor which was then hydrated in PBS for 1.5h at 60°C to obtain drug encapsulated self-assembled liposomes. The unencapsulated free drug was filtered using G-25 sephadex column. Later the eluted liposomes were extruded using a 200 nm polycarbonate filter membrane to obtain nanoparticles of desired size. The drug encapsulation efficiency was identified using UV-Vis spectrophotometry and the size as well as zeta potential were determined using Malvern Zetasizer Nano ZS90.

Characterization of Nanoparticles

For stability studies, the nanoparticles were incubated either in PBS at 4°C or in 10% human serum at room temperature for extended duration of time. PBS stability is for storage conditions, whereas serum stability is for physiological conditions. While incubating in respective buffers, the nanoparticles were assessed for their size and surface charge at indicated time points. Additionally, their morphology and size were confirmed via Cryo-TEM performed by the UMASS Chan Medical School Core Facility.

Cellular uptake of FITC encapsulated nanoparticles

For internalization studies, nanoparticles were encapsulated with FITC, fluorescein isothiocyanate at 5 mol percent, to obtain fluorescent nanoparticles for internalization studies. For concentration dependent studies, the immortalized macrophages were incubated with fluorescent nanoparticles ranging from 0.1 to 10 mM for 4 hours, and the fluorescence intensity was recorded using flow cytometry. For time dependent studies, the cells were incubated with fluorescent nanoparticles for different time points 0h, 2h, 4h and 8h, followed

by NucBlue staining in order to stain the nuclei. Further, the cells were images using Crest V2 spinning disk and the fluorescence intensity was measured using NIS Elements V6.2.

Cell culture, NLRP3 stimulation and drug treatment

Immortalized macrophages were utilized for all the in-vitro assays. They were cultured in complete DMEM containing 10% FBS and 1% Pen-Strep. For NLRP3 stimulation, the cells were first primed using ultrapure LPS for 2h in order to activate signal 1 and then they were treated with 10 mM nigericin for ½ to 1h for signal 2. Free drug or nanoparticle treatments were performed in between signal 1 and signal 2 for indicated time points.

LPS induced Peritonitis Sepsis Model

All the animal protocols were approved by IACUC (Institutional Animal Care Use Committees), at University of Massachusetts, Amherst. Female C57BL/6 mice of age 6-8 weeks were procured from Charles River and housed in a pathogen free environment under 12 hours light or dark cycles. For establishing LPS Peritonitis Sepsis Model, mice were first injected with pure LPS intraperitoneally. This was followed by intravenous I.V. injection of nanoparticles or free drugs after 1h of LPS injections. For injections nanoparticles as well as MCC-950 free drug was reconstituted in ultrapure PBS, whereas disulfiram was reconstituted in sesame oil. After all the injections, the mice were very closely monitored for weight, mobility, posture, appearance, and survival. All the mice were humanely sacrificed by following the rules set in the animal protocol, in compliance with the IACUC. Immediately after sacrificing the mice, their blood was collected with cardiac puncture and peritoneal cells were collected by rinsing the peritoneal cavity with ice cold PBS containing 3% FBS. Peritoneal cells were then lysed using RIPA buffer to isolate the total protein. Additionally, all the tissues were harvested and fixed in formalin. All the animal procedures were performed in accordance with the institutional guidelines for using and careful handling of laboratory animals of the University of Massachusetts, Amherst, MA, USA and all the procedures were approved by the Animal Ethics Committee of the University of Massachusetts Amherst.

ELISA

IL-1β ELISA was performed according to the manufacturer's protocol using the ThermoFisher IL-1 beta mouse uncoated ELISA kit. For in-vitro assays, it was performed in cell supernatant by diluting them 1X ELISPOT, whereas for in-vivo assays, isolated serum was utilized. For all the ELISAs the sample was incubated overnight at 4°C to allow maximum binding.

Immunoblotting

For both in-vitro and in-vivo assays, protein was isolated by cell lysis using RIPA buffer enriched with 1X protease inhibitor. For in-vitro, both the cell lysate and supernatant were used for immunoblotting. For in-vivo, total protein was isolated from peritoneal cells immediately after their isolation. The protein was quantified using BCA assay and an equal amount of protein was loaded onto gels. For in-vitro samples, we performed regular western protein using 10% polyacrylamide gels and wet transfer on PVDF membrane. Later the membrane was blocked in 5% skim milk and stained with respective primary and secondary antibodies prepared in TBST. Whereas for in-vivo, we chose to use protein simple Wes, due to very limited sample quantity. The manufacturer's protocol was utilized for loading the plate and carrying out the assay.

Hematoxylin & Eosin (H&E) Staining for Biosafety/Toxicity.

Tissues from the vital organs (liver, spleen, kidney, lung and heart) were collected at the termination, which were then fixed in 10% neutral buffered formalin for 24h, decanted and stored in 70% ethanol for long term at 4 degrees Celsius. The samples were then transported to Biospecimen Resource and Molecular Analysis Facility (BRaMA), PVLSI, UMass Chan Medical-Baystate, where they were paraffin embedded, sectioned at 5 μM thickness and H&E stained. Analysis was performed by the residents from Department of Pathology, UMass Chan Medical School at Bay State Health, Springfield, MA.

Statistical Analysis

GraphPad Prism 10 was utilized to analyze statistics. For two groups comparison, two-tailed unpaired t-test was utilized whereas for multiple groups, ordinary one-way or two-way ANOVA was performed followed by Dunnett's or Sidak's multiple comparisons. Results were represented as either mean ± s.e.m. (standard error of mean) or mean ± s.d. (standard deviation). P-value less than 0.05 was considered as significant.

SUPPORTING INFORMATION

The supporting information is available free of charge on the Publications website.

Description of materials and Supporting Figures S1-S7

AUTHOR CONTRIBUTIONS

A.K. conceived the idea and mentored the research; D. N. and A. K. designed the experiments; D.N., M. D., J.F. III and A. P. performed the experiments; D. N., M D., J. F. III and A. K. wrote the paper and received comments from all the authors. All authors have given approval to the final version of the manuscript.

CONFLICTS OF INTEREST

The authors declare no competing financial interests.

ACKNOWLEDGMENT

This work was financially supported by the National Science Foundation CAREER Award (2142917) to A. K. This work was supported in part by a Fellowship from the University of Massachusetts to J. Forster

III as part of the Biotechnology Training Program (National Research Service Award T32 GM135096). We would like to thank the Biophysical Characterization Core at the Institute for Applied Life Sciences (IALS), the University of Massachusetts Amherst, for lending their expertise in regard to characterization experiments. We would also like to thank the Light Microscopy Core Facility at the University of Massachusetts Amherst for their help and consultation while performing confocal imaging. All institutional and national guidelines for the care and use of laboratory animals were followed and approved by the University of Massachusetts Amherst Institutional Use and Care of Animals Committee. All the visual figures were created with Biorender.com.

REFERENCES:

(1) van der Poll, T.; Shankar-Hari, M.; Wiersinga, W. J. The Immunology of Sepsis. *Immunity* **2021**, *54* (11), 2450–2464. https://doi.org/10.1016/j.immuni.2021.10.012.

(2) Delano, M. J.; Ward, P. A. Sepsis-Induced Immune Dysfunction: Can Immune Therapies Reduce Mortality? *J. Clin. Invest. 126* (1), 23–31. https://doi.org/10.1172/JCI82224.

(3) De Backer, D.; Cecconi, M.; Lipman, J.; Machado, F.; Myatra, S. N.; Ostermann, M.; Perner, A.; Teboul, J.-L.; Vincent, J.-L.; Walley, K. R. Challenges in the Management of Septic Shock: A Narrative Review. *Intensive Care Med.* **2019**, *45* (4), 420–433. https://doi.org/10.1007/s00134-019-05544-x.

(4) Ulloa, L.; Brunner, M.; Ramos, L.; Deitch, E. A. Scientific and Clinical Challenges in Sepsis. *Curr. Pharm. Des.* **2009**, *15* (16), 1918–1935.

(5) Schultz, M. J.; Dünser, M. W.; Dondorp, A. M.; Adhikari, N. K. J.; Iyer, S.; Kwizera, A.; Lubell, Y.; Papali, A.; Pisani, L.; Riviello, E. D.; Angus, D. C.; Azevedo, L. C.; Baker, T.; Diaz, J. V.; Festic, E.; Haniffa, R.; Jawa, R.; Jacob, S. T.; Kissoon, N.; Lodha, R.; Martin-Loeches, I.; Lundeg, G.; Misango, D.; Mer, M.; Mohanty, S.; Murthy, S.; Musa, N.; Nakibuuka, J.; Neto, A. S.; Mai, N. H.; Thien, B. N.; Pattnaik, R.; Phua, J.; Preller, J.; Povoa, P.; Ranjit, S.; Talmor, D.; Thevanayagam, J.; Thwaites, C. L. Current Challenges in the Management of Sepsis in ICUs in Resource-Poor Settings and Suggestions for the Future.

In *Sepsis Management in Resource-limited Settings*; Dondorp, A. M., Dünser, M. W., Schultz, M. J., Eds.; Springer International Publishing: Cham, 2019; pp 1–24. https://doi.org/10.1007/978-3-030-03143-5_1.

(6) Delano, M. J.; Ward, P. A. The Immune System's Role in Sepsis Progression, Resolution and Long-Term Outcome. *Immunol. Rev.* **2016**, *274* (1), 330–353. https://doi.org/10.1111/imr.12499.

(7) Hotchkiss, R. S.; Coopersmith, C. M.; McDunn, J. E.; Ferguson, T. A. Tilting toward Immunosuppression. *Nat. Med.* **2009**, *15* (5), 496–497. https://doi.org/10.1038/nm0509-496.

(8) Shi, X.; Tan, S.; Tan, S. NLRP3 Inflammasome in Sepsis (Review). *Mol. Med. Rep.* **2021**, *24* (1), 1–8. https://doi.org/10.3892/mmr.2021.12153.

(9) Boomer, J. S.; Green, J. M.; Hotchkiss, R. S. The Changing Immune System in Sepsis. *Virulence* **2014**, *5* (1), 45–56. https://doi.org/10.4161/viru.26516.

(10) Steinhagen, F.; Schmidt, S. V.; Schewe, J.-C.; Peukert, K.; Klinman, D. M.; Bode, C. Immunotherapy in Sepsis - Brake or Accelerate? *Pharmacol. Ther.* **2020**, *208*, 107476. https://doi.org/10.1016/j.pharmthera.2020.107476.

(11) Danielski, L. G.; Giustina, A. D.; Bonfante, S.; Barichello, T.; Petronilho, F. The NLRP3 Inflammasome and Its Role in Sepsis Development. *Inflammation* **2020**, *43* (1), 24–31. https://doi.org/10.1007/s10753-019-01124-9.

(12) Cornelius, D. C.; Travis, O. K.; Tramel, R. W.; Borges-Rodriguez, M.; Baik, C. H.; Greer, M.; Giachelli, C. A.; Tardo, G. A.; Williams, J. M. NLRP3 Inflammasome Inhibition Attenuates Sepsis-Induced Platelet Activation and Prevents Multi-Organ Injury in Cecal-Ligation Puncture. *PLoS ONE* **2020**, *15* (6), e0234039. https://doi.org/10.1371/journal.pone.0234039.

(13) Mao, K.; Chen, S.; Chen, M.; Ma, Y.; Wang, Y.; Huang, B.; He, Z.; Zeng, Y.; Hu, Y.; Sun, S.; Li, J.; Wu, X.; Wang, X.; Strober, W.; Chen, C.; Meng, G.; Sun, B. Nitric Oxide Suppresses NLRP3 Inflammasome Activation and Protects against LPS-Induced Septic Shock. *Cell Res.* **2013**, *23* (2), 201–212. https://doi.org/10.1038/cr.2013.6.

(14) Swanson, K. V.; Deng, M.; Ting, J. P.-Y. The NLRP3 Inflammasome: Molecular Activation and Regulation to Therapeutics. *Nat. Rev. Immunol.* **2019**, *19* (8), 477–489. https://doi.org/10.1038/s41577-019-0165-0.

(15) Kelley, N.; Jeltema, D.; Duan, Y.; He, Y. The NLRP3 Inflammasome: An Overview of Mechanisms of Activation and Regulation. *Int. J. Mol. Sci.* **2019**, *20* (13). https://doi.org/10.3390/ijms20133328.

(16) Xu, J.; Núñez, G. The NLRP3 Inflammasome: Activation and Regulation. *Trends Biochem. Sci.* **2023**, *48* (4), 331–344. https://doi.org/10.1016/j.tibs.2022.10.002.

(17) He, Y.; Hara, H.; Núñez, G. Mechanism and Regulation of NLRP3 Inflammasome Activation. *Trends Biochem. Sci.* **2016**, *41* (12), 1012–1021. https://doi.org/10.1016/j.tibs.2016.09.002.

(18) Nandi, D.; Farid, N. S. S.; Karuppiah, H. A. R.; Kulkarni, A. Imaging Approaches to Monitor Inflammasome Activation. *J. Mol. Biol.* **2022**, *434* (4), 167251. https://doi.org/10.1016/j.jmb.2021.167251.

(19) Zhang, X.; Xu, A.; Lv, J.; Zhang, Q.; Ran, Y.; Wei, C.; Wu, J. Development of Small Molecule Inhibitors Targeting NLRP3 Inflammasome Pathway for Inflammatory Diseases. *Eur. J. Med. Chem.* **2020**, *185*, 111822. https://doi.org/10.1016/j.ejmech.2019.111822.

(20) Zahid, A.; Li, B.; Kombe, A. J. K.; Jin, T.; Tao, J. Pharmacological Inhibitors of the NLRP3 Inflammasome. *Front. Immunol.* **2019**, *10*.

(21) Batiha, G. E.-S.; Al-Gareeb, A. I.; Rotimi, D.; Adeyemi, O. S.; Al-kuraishy, H. M. Common NLRP3 Inflammasome Inhibitors and Covid-19: Divide and Conquer. *Sci. Afr.* **2022**, *18*, e01407. https://doi.org/10.1016/j.sciaf.2022.e01407.

(22) Patra, J. K.; Das, G.; Fraceto, L. F.; Campos, E. V. R.; Rodriguez-Torres, M. del P.; Acosta-Torres, L. S.; Diaz-Torres, L. A.; Grillo, R.; Swamy, M. K.; Sharma, S.; Habtemariam, S.; Shin, H.-S. Nano Based Drug Delivery Systems: Recent Developments and Future Prospects. *J. Nanobiotechnology* **2018**, *16* (1), 71. https://doi.org/10.1186/s12951-018-0392-8.

(23) Wang, H.; Zhou, Y.; Sun, Q.; Zhou, C.; Hu, S.; Lenahan, C.; Xu, W.; Deng, Y.; Li, G.; Tao, S. Update on Nanoparticle-Based Drug Delivery System for Anti-Inflammatory Treatment. *Front. Bioeng. Biotechnol.* **2021**, *9*, 630352. https://doi.org/10.3389/fbioe.2021.630352.

(24) Placha, D.; Jampilek, J. Chronic Inflammatory Diseases, Anti-Inflammatory Agents and Their Delivery Nanosystems. *Pharmaceutics* **2021**, *13* (1), 64. https://doi.org/10.3390/pharmaceutics13010064.

(25) *Sepsis and septic shock | Nature Reviews Disease Primers*. https://www.nature.com/articles/nrdp201645 (accessed 2023-09-30).

(26) *Inflammation and Coagulation: Implications for the Septic Patient | Clinical Infectious Diseases | Oxford Academic*. https://academic.oup.com/cid/article/36/10/1259/307497 (accessed 2023-09-30).

(27) Fujishima, S. Organ Dysfunction as a New Standard for Defining Sepsis. *Inflamm. Regen.* **2016**, *36* (1), 24. https://doi.org/10.1186/s41232-016-0029-y.

(28) Cross, A. S.; Opal, S. M. A New Paradigm for the Treatment of Sepsis: Is It Time To Consider Combination Therapy? *Ann. Intern. Med.* **2003**, *138* (6), 502–505. https://doi.org/10.7326/0003-4819-138-6-200303180-00016.

(29) Upadhyay, K.; Hiregoudar, B.; Meals, E.; English, B. K.; Talati, A. J. Combination Therapy with Ampicillin and Azithromycin Improved Outcomes in a Mouse Model of Group B Streptococcal Sepsis. *PLOS ONE* **2017**, *12* (7), e0182023. https://doi.org/10.1371/journal.pone.0182023.

(30) Vazquez-Grande, G.; Kumar, A. Optimizing Antimicrobial Therapy of Sepsis and Septic Shock: Focus on Antibiotic Combination Therapy. *Semin. Respir. Crit. Care Med.* **2015**, *36* (1), 154–166. https://doi.org/10.1055/s-0034-1398742.

(31) Patra, J. K.; Das, G.; Fraceto, L. F.; Campos, E. V. R.; Rodriguez-Torres, M. del P.; Acosta-Torres, L. S.; Diaz-Torres, L. A.; Grillo, R.; Swamy, M. K.; Sharma, S.; Habtemariam, S.; Shin, H.-S. Nano Based Drug Delivery Systems: Recent Developments and Future Prospects. *J. Nanobiotechnology* **2018**, *16* (1), 71. https://doi.org/10.1186/s12951-018-0392-8.

(32) Rizvi, S. A. A.; Saleh, A. M. Applications of Nanoparticle Systems in Drug Delivery Technology. *Saudi Pharm. J. SPJ* **2018**, *26* (1), 64–70. https://doi.org/10.1016/j.jsps.2017.10.012.

(33) Gelperina, S.; Kisich, K.; Iseman, M. D.; Heifets, L. The Potential Advantages of Nanoparticle Drug Delivery Systems in Chemotherapy of Tuberculosis. *Am. J. Respir. Crit. Care Med.* **2005**, *172* (12), 1487–1490. https://doi.org/10.1164/rccm.200504-613PP.

(34) Perera, A. P.; Fernando, R.; Shinde, T.; Gundamaraju, R.; Southam, B.; Sohal, S. S.; Robertson, A. A. B.; Schroder, K.; Kunde, D.; Eri, R. MCC950, a Specific Small Molecule Inhibitor of NLRP3 Inflammasome Attenuates Colonic Inflammation in Spontaneous Colitis Mice. *Sci. Rep.* **2018**, *8*, 8618. https://doi.org/10.1038/s41598-018-26775-w.

(35) *Engineering precision nanoparticles for drug delivery | Nature Reviews Drug Discovery*. https://www.nature.com/articles/s41573-020-0090-8 (accessed 2023-09-14).

(36) Ramesh, A.; Kumar, S.; Nandi, D.; Kulkarni, A. CSF1R- and SHP2-Inhibitor-Loaded Nanoparticles Enhance Cytotoxic Activity and Phagocytosis in Tumor-Associated Macrophages. *Adv. Mater. Deerfield Beach Fla* **2019**, *31* (51), e1904364. https://doi.org/10.1002/adma.201904364.

(37) Hald Albertsen, C.; Kulkarni, J. A.; Witzigmann, D.; Lind, M.; Petersson, K.; Simonsen, J. B. The Role of Lipid Components in Lipid Nanoparticles for Vaccines and Gene Therapy. *Adv. Drug Deliv. Rev.* **2022**, *188*, 114416. https://doi.org/10.1016/j.addr.2022.114416.

(38) Strachan, J. B.; Dyett, B. P.; Nasa, Z.; Valery, C.; Conn, C. E. Toxicity and Cellular Uptake of Lipid Nanoparticles of Different Structure and Composition. *J. Colloid Interface Sci.* **2020**, *576*, 241–251. https://doi.org/10.1016/j.jcis.2020.05.002.

(39) Coll, R. C.; Robertson, A. A. B.; Chae, J. J.; Higgins, S. C.; Muñoz-Planillo, R.; Inserra, M. C.; Vetter, I.; Dungan, L. S.; Monks, B. G.; Stutz, A.; Croker, D. E.; Butler, M. S.; Haneklaus, M.; Sutton, C. E.; Núñez, G.; Latz, E.; Kastner, D. L.; Mills, K. H. G.; Masters, S. L.; Schroder, K.; Cooper, M. A.; O'Neill, L. A. J. A Small-Molecule Inhibitor of the NLRP3 Inflammasome for the Treatment of Inflammatory Diseases. *Nat. Med.* **2015**, *21* (3), 248–255. https://doi.org/10.1038/nm.3806.

(40) van der Heijden, T.; Kritikou, E.; Venema, W.; van Duijn, J.; van Santbrink, P. J.; Slütter, B.; Foks, A. C.; Bot, I.; Kuiper, J. NLRP3 Inflammasome Inhibition by MCC950 Reduces Atherosclerotic Lesion Development in Apolipoprotein E–Deficient Mice—Brief Report. *Arterioscler. Thromb. Vasc. Biol.* **2017**, *37* (8), 1457–1461. https://doi.org/10.1161/ATVBAHA.117.309575.

(41) Walle, L. V.; Stowe, I. B.; Šácha, P.; Lee, B. L.; Demon, D.; Fossoul, A.; Hauwermeiren, F. V.; Saavedra, P. H. V.; Šimon, P.; Šubrt, V.; Kostka, L.; Stivala, C. E.; Pham, V. C.; Staben, S. T.; Yamazoe, S.; Konvalinka, J.; Kayagaki, N.; Lamkanfi, M. MCC950/CRID3 Potently Targets the NACHT Domain of Wild-Type NLRP3 but Not Disease-Associated Mutants for Inflammasome Inhibition. *PLOS Biol.* **2019**, *17* (9), e3000354. https://doi.org/10.1371/journal.pbio.3000354.

(42) Perera, A. P.; Fernando, R.; Shinde, T.; Gundamaraju, R.; Southam, B.; Sohal, S. S.; Robertson, A. A. B.; Schroder, K.; Kunde, D.; Eri, R. MCC950, a Specific Small Molecule Inhibitor of NLRP3 Inflammasome Attenuates Colonic Inflammation in Spontaneous Colitis Mice. *Sci. Rep.* **2018**, *8*, 8618. https://doi.org/10.1038/s41598-018-26775-w.

(43) Hu, J. J.; Liu, X.; Xia, S.; Zhang, Z.; Zhang, Y.; Zhao, J.; Ruan, J.; Luo, X.; Lou, X.; Bai, Y.; Wang, J.; Hollingsworth, L. R.; Magupalli, V. G.; Zhao, L.; Luo, H. R.; Kim, J.; Lieberman, J.; Wu, H. FDA-Approved Disulfiram Inhibits Pyroptosis by Blocking Gasdermin D Pore Formation. *Nat. Immunol.* **2020**, *21* (7), 736–745. https://doi.org/10.1038/s41590-020-0669-6.

(44) Sborgi, L.; Rühl, S.; Mulvihill, E.; Pipercevic, J.; Heilig, R.; Stahlberg, H.; Farady, C. J.; Müller, D. J.; Broz, P.; Hiller, S. GSDMD Membrane Pore Formation Constitutes the Mechanism of Pyroptotic Cell Death. *EMBO J.* **2016**, *35* (16), 1766–1778. https://doi.org/10.15252/embj.201694696.

(45) Wang, C.; Yang, T.; Xiao, J.; Xu, C.; Alippe, Y.; Sun, K.; Kanneganti, T.-D.; Monahan, J. B.; Abu-Amer, Y.; Lieberman, J.; Mbalaviele, G. NLRP3 Inflammasome Activation Triggers Gasdermin D-Independent Inflammation. *Sci. Immunol.* **2021**, *6* (64), eabj3859. https://doi.org/10.1126/sciimmunol.abj3859.

(46) He, W.; Wan, H.; Hu, L.; Chen, P.; Wang, X.; Huang, Z.; Yang, Z.-H.; Zhong, C.-Q.; Han, J. Gasdermin D Is an Executor of Pyroptosis and Required for Interleukin-1β Secretion. *Cell Res.* **2015**, *25* (12), 1285–1298. https://doi.org/10.1038/cr.2015.139.

(47) Zhang, H. Thin-Film Hydration Followed by Extrusion Method for Liposome Preparation. *Methods Mol. Biol. Clifton NJ* **2017**, *1522*, 17–22. https://doi.org/10.1007/978-1-4939-6591-5_2.

(48) Xu, L.; Wang, X.; Liu, Y.; Yang, G.; Falconer, R. J.; Zhao, C.-X. Lipid Nanoparticles for Drug Delivery. *Adv. NanoBiomed Res.* **2022**, *2* (2), 2100109. https://doi.org/10.1002/anbr.202100109.

(49) *Nanoreporter for Real-Time Monitoring of Inflammasome Activity and Targeted Therapy - PubMed*. https://pubmed.ncbi.nlm.nih.gov/36603165/ (accessed 2023-10-02).

(50) Sand, J.; Haertel, E.; Biedermann, T.; Contassot, E.; Reichmann, E.; French, L. E.; Werner, S.; Beer, H.-D. Expression of Inflammasome Proteins and Inflammasome Activation Occurs in Human, but Not in Murine Keratinocytes. *Cell Death Dis.* **2018**, *9* (2), 1–14. https://doi.org/10.1038/s41419-017-0009-4.

(51) Stutz, A.; Horvath, G. L.; Monks, B. G.; Latz, E. ASC Speck Formation as a Readout for Inflammasome Activation. *Methods Mol. Biol. Clifton NJ* **2013**, *1040*, 91–101. https://doi.org/10.1007/978-1-62703-523-1_8.

(52) Nagar, A.; Rahman, T.; Harton, J. A. The ASC Speck and NLRP3 Inflammasome Function Are Spatially and Temporally Distinct. *Front. Immunol.* **2021**, *12*.

(53) Nandi, D.; Shivrayan, M.; Gao, J.; Krishna, J.; Das, R.; Liu, B.; Thayumanavan, S.; Kulkarni, A. Core Hydrophobicity of Supramolecular Nanoparticles Induces NLRP3 Inflammasome Activation. *ACS Appl. Mater. Interfaces* **2021**, *13* (38), 45300–45314. https://doi.org/10.1021/acsami.1c14082.

(54) Iii, J. F.; Nandi, D.; Kulkarni, A. mRNA-Carrying Lipid Nanoparticles That Induce Lysosomal Rupture Activate NLRP3 Inflammasome and Reduce mRNA Transfection Efficiency. *Biomater. Sci.* **2022**, *10* (19), 5566–5582. https://doi.org/10.1039/D2BM00883A.

(55) Debnath, M.; Forster, J. I.; Ramesh, A.; Kulkarni, A. Protein Corona Formation on Lipid Nanoparticles Negatively Affects the NLRP3 Inflammasome Activation. *Bioconjug. Chem.* **2023**. https://doi.org/10.1021/acs.bioconjchem.3c00329.